Cavity-ring-down Doppler-broadening primary thermometry

Riccardo Gotti,[1] Luigi Moretti,[2] Davide Gatti,[1] Antonio Castrillo,[2] Gianluca Galzerano,[1]
Paolo Laporta,[1] Livio Gianfrani,[2] and Marco Marangoni[1]

[1]*Politecnico di Milano and IFN-CNR, Via G. Previati 1/C, 23900 Lecco, Italy*

[2]*Università degli Studi della Campania "Luigi Vanvitelli"–Dipartimento di Matematica e Fisica, Viale Lincoln 5, 81100 Caserta, Italy*

(Received 14 September 2017; published 25 January 2018)

A step forward in Doppler-broadening thermometry is demonstrated using a comb-assisted cavity-ring-down spectroscopic approach applied to an isolated near-infrared line of carbon dioxide at thermodynamic equilibrium. Specifically, the line-shape of the $P_e(12)$ line of the (30012) ← (00001) band of CO_2 at 1.578 μm is accurately measured and its Doppler width extracted from a refined multispectrum fitting procedure accounting for the speed dependence of the relaxation rates, which were found to play a role even at the very low pressures explored, from 1 to 7 Pa. The thermodynamic gas temperature is retrieved with relative uncertainties of 8×10^{-6} (type A) and 11×10^{-6} (type B), which ranks the system at the first place among optical methods. Thanks to a measurement time of only ≈5 h, the technique represents a promising pathway toward the optical determination of the thermodynamic temperature with a global uncertainty at the 10^{-6} level.

DOI: 10.1103/PhysRevA.97.012512

The forthcoming redefinition of the unit kelvin [1], in 2018, in terms of a fixed value of the Boltzmann constant, prompts the interest for primary thermometers that are capable to operate over a relatively large part of the temperature scale with very high accuracy. Among primary methods, important advancements [2] have been obtained over the past decade on dielectric constant gas thermometry and Johnson noise thermometry [3,4]. After a first successful experiment of Doppler-broadening thermometry (DBT) [5], followed by significant improvements [6,7], the international community of fundamental metrology recognized the importance of an optical method that links the thermodynamic temperature to an optical frequency, as an independent confirmation of other primary approaches.

DBT consists of retrieving the Doppler width $\Delta\nu_D$ from the highly accurate observation of the shape of a given atomic or molecular line, in a laser-based absorption-spectroscopy experiment under a linear regime of radiation–matter interaction [8]. Once $\Delta\nu_D$ is measured, if the central frequency (ν_0) and the atomic or molecular mass (M) are known, the inversion of the well-known equation $\Delta\nu_D = \frac{\nu_0}{c}\sqrt{8 \ln 2 \frac{k_B T}{M}}$ allows one to determine the thermal energy and, consequently, either the gas temperature (T) or the Boltzmann constant (k_B). So far, the most accurate implementation of DBT has been performed on a rovibrational transition of a water isotopologue at 1.39 μm. Using a dual-laser spectrometer and adopting a very sophisticated spectral analysis procedure, the Boltzmann constant could be determined with a combined uncertainty of 24 parts per million (ppm) [6,9,10].

The history of DBT [11] shows that the major hurdle for a low-uncertainty determination of the Doppler width and hence of the thermal energy is the choice of the line-shape model adopted for the spectral analysis. Since a fully *ab initio* line-shape calculation is prohibitively complex for self-colliding molecules, a model suitable for being implemented into a fitting routine requires approximations and simplifications. At the same time, the model must be sophisticated enough to account for various collisional effects [12]. A way to overcome these difficulties, while preserving the advantage of a near-infrared spectral range where the linearity of detectors is well assessed [11], is to resort to a highly sensitive detection technique, such as cavity-ring-down spectroscopy (CRDS), enabling the investigation of few-Pascal Doppler regimes and the use of simplified line-shape models. This approach has been recently pursued by Hu *et al.*, by recording acetylene spectra at 787 nm at 1.5 Pa [13]. Nevertheless, their thermometer showed a large systematical deviation (800 ppm) as attributed to weak lines overlapped with the selected transition.

This work, taking full advantage of the CRDS potential, tackles in a global way the reduction of the uncertainty budget in a DBT experiment, through a proper choice of gas sample, pressure regime, calibration of the horizontal and vertical axis of the measurement, line-shape modeling, and fitting procedure. The molecular target is pure carbon dioxide, which is an excellent choice as it is a centrosymmetric linear molecule with only three fundamental vibrations exhibiting a simplified infrared spectrum as compared to other polyatomic molecules. Moreover, its spectral lines do not present any hyperfine structure, while the lack of a permanent dipole moment reduces significantly the interactions with the walls of the gas container [11]. Specifically, a weak overtone line of CO_2 is probed around 1.578 μm at a pressure of a few Pascal by means of a highly sensitive CRDS spectrometer referenced to an optical frequency comb, affording a very favorable combination of sensitivity, frequency calibration, and dense frequency grid. Together with a multispectrum fitting procedure applied to a large set of spectra at different pressures, this results in a statistical uncertainty of 8 ppm over a measurement time of 5 h, 40 times shorter than the golden standard for DBT [6]. As this couples with an 11.5-ppm systematic uncertainty, mainly related to the choice of the line-shape model, the combined uncertainty

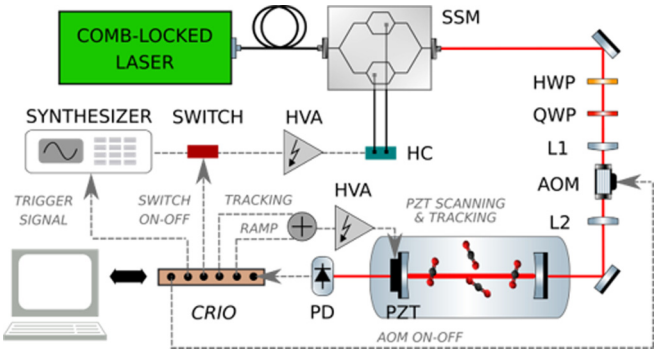

FIG. 1. Experimental setup. SSM, single-sideband-modulator; L1,2, lenses; HWP (QWP), half- (quarter-) wave plate; AOM, acousto-optic modulator; HVA, high-voltage amplifier; HC, 90° hybrid coupler; PZT, piezoelectric transducer; PD, photodetector; CRIO, compact reconfigurable input-output board. Solid lines, optical beams. Dashed line, electrical connections.

in the determination of the gas temperature amounts to 14 ppm, which represent a leap forward by a factor of 2 with respect to the state of the art of molecular samples [6] and by a factor of 4 with respect to that of atomic targets [7].

The optical lay-out of the spectrometer, sketched in Fig. 1, minimizes some of the major sources of uncertainties in DBT. The 1.5–1.63 μm spectral range covers well-known combination vibrational bands of CO_2 and matches the telecom spectral window where lasers, detectors and optics are available with high quality. The requirement of a high signal-to-noise-ratio (SNR) at few-Pascal pressures with line strengths of $\approx 10^{-23}$ cm/molecule is fulfilled by an enhancement cavity with a finesse of 125 000 and a free-spectral-range of 300 MHz. The intracavity absorption is extracted by CRDS, which benefits from a minimal sensitivity to laser intensity noise and to frequency-to-amplitude noise conversion; moreover, it offers excellent linearity over a large dynamic range since it relies on a relative measurement of cavity-photon-lifetime rather than on the determination of an absorption depth. Using a high-finesse cavity implies the need to bring a narrow cavity mode into coincidence with the laser frequency, which results in a time-consuming cavity-length adjustment if a high number of spectral points are targeted to achieve an accurate modeling of the absorption profile and correspondingly reduce systematic deviations. We solved this trade-off by combining a dither-based locking of the cavity to the laser with a fast and agile scanning of the laser through an optical single-sideband modulator (SSM) [14,15]. The piezo-dithering is performed at 500 Hz over ± 8.3 MHz and ensures a 1-kHz ring-down (RD) rate. The single sideband is quickly stepped by 300 MHz from a cavity mode to the next one over a span of 4.2 GHz (≈12 times the Doppler width) without the need for cavity length adjustment apart from a compensation for small cavity drifts; once the stepping is completed, the single sideband is detuned by a few MHz (within the capture range of the dither locking) and then stepped back across the cavity modes to provide an interleaved spectrum. Back-and-forth frequency scans are repeated till a uniform distribution of points over 4.2 GHz is obtained: interestingly, this results in an acquisition time of only 6.4 s for a 3200-points spectrum with 2 RD times per spectral point. An even number of RD times is required to average out the effect of the Doppler shift given by the moving mirror (see discussion below). Typically, a higher (yet even) number of RD times is chosen for the central part of the absorption spectrum to not degrade the SNR when the RD time is reduced. On the spectra wings, where the RD time is 64 μs, the noise level with a 2-ms acquisition time per spectral point is $9.8 \times 10^{-11}\,\mathrm{cm}^{-1}$ (see Ref. [16] for a sensitivity analysis).

To achieve a highly repeatable frequency axis and average consecutive spectra, the probe laser is frequency locked to a 100-MHz self-referenced Er:fiber frequency comb whose repetition frequency is calibrated against a GPS-disciplined Rb reference through interposition of a quartz oscillator. This gives a stability of 1.8×10^{-12} over the 17 s required for the acquisition of a single spectrum with a nonuniform distribution of RD times. On the thermodynamic side, the cavity is sandwiched between two massive aluminum shells actively kept by stripe heaters at a temperature around 298.5 K, as read out with a resolution of 0.1 mK by a set of PT100 sensors calibrated within 25 mK. The temperature stability is 3 mK rms. The temperature uniformity is at the same level and it is ensured by the high thermal conductivity of aluminum combined with air-recirculation within the enclosure box.

Spectroscopic measurements were focused on the $P_e(12)$ line of the 30012-00001 band of CO_2, centered at $6337.990396\,\mathrm{cm}^{-1}$ with strength of 1.512×10^{-23} cm/molecule (HITRAN data, [17]). The explored pressure range goes from 1 to 7.3 Pa, corresponding to peak absorption values from 2.7×10^{-7} to $1.6 \times 10^{-6}\ \mathrm{cm}^{-1}$. In these conditions the Doppler width (353 MHz) dominates by more than three orders of magnitude with respect to the collisional contribution. The measurements were performed at 33 different pressure values over several days for a reliable reproducibility check. Each measurement encompasses 35 consecutive profiles acquired in ≈10 min. By subdividing each measurement in 7 groups and by averaging together the 5 profiles of each group, 7 spectra were obtained at each pressure: this allowed to organize the overall ensemble of spectroscopic data in 7 data sets, each one composed of 33 spectra, as many as the pressure values. Figure 2 reports an example of those spectra at different pressures: the zoomed-in views highlight an rms noise level of $4.3 \times 10^{-11}\,\mathrm{cm}^{-1}$ on the spectral wings and a 1.3-MHz spacing between adjacent points. The residuals obtained from the multiple-fitting procedure described below are substantially flat and featureless: a slightly higher noise pedestal is visible at the center of the spectrum, due to the shorter ring-down times and to correspondingly lower SNR. Etalon effects are barely visible thanks to an efficient suppression by fringe scrambling [16]: moreover, as their free-spectral-range is much smaller than the absorption linewidth, they negligibly impact on the fitting quality.

The choice of the line-shape model was influenced by the need to include the collisional width and its speed dependence, despite it being smaller than 1 MHz. In fact, individual fits with a Gaussian function returned an unphysical dependence of the retrieved Doppler width on pressure, showing that a simplified description was unsatisfactory. For this reason, we decided to start from the partially correlated quadratic speed-dependent hard-collision profile, a widely recognized model for high-resolution spectroscopy. It is sufficiently sophisticated to

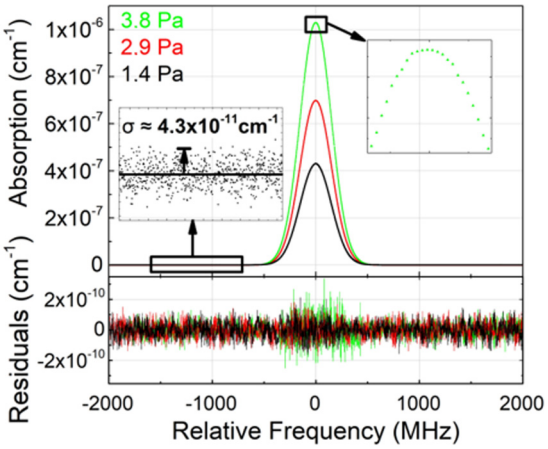

FIG. 2. Averaged spectra at different pressures. Each spectrum is the average of five consecutive profiles. Insets highlight vertical and horizontal resolution. The bottom panel reports the residuals obtained from a Multiple Fitting Procedure with a speed-dependent Voigt profile.

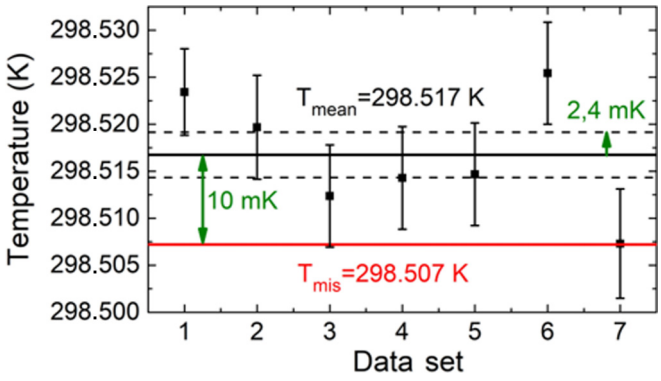

FIG. 3. Absolute temperature given by the CRDS thermometer for each data set, as retrieved by MFP. The mean temperature of 298.517 K is offset by 10 mK (33 ppm) from the PT100 reading (red line). The weighted mean is affected by an uncertainty of 8 ppm (2.4 mK).

capture various collisional perturbations to the isolated line-shape [18–21], but at the same time, thanks to the implementation provided by Ngo *et al.* [22], it requires a small computation effort and may efficiently be integrated into a fitting routine. We will hereafter refer to it as Hartmann-Tran profile (HTP). Under the quadratic approximation for the collisional width (Γ) and shift (Δ), the complex dephasing collision frequency $\Gamma + i\Delta$ is expressed as a function of the square of the molecular speed v according to the formula

$$\Gamma(v) + i\Delta(v) = (\Gamma_0 + i\Delta_0) + (\Gamma_2 + i\Delta_2)\left[\left(\frac{v}{\tilde{v}}\right)^2 - \frac{3}{2}\right], \tag{1}$$

where $\tilde{v} = \sqrt{2k_BT/M}$ is the most probable speed, Γ_0 and Δ_0 are the collisional width and shift averaged over all molecular speeds, Γ_2 and Δ_2 are the quadratic contributions linearly related to Γ_0 and Δ_0 through the equations $\Gamma_2 = a_W\Gamma_0$ and $\Delta_2 = a_S\Delta_0$, with a_W and a_S depending on the specific intermolecular potential [23]. The HTP line-shape, $F_{\mathrm{HTP}}(\omega)$, as a function of the angular frequency ω and with Γ/Δ parameters given by Eq. (1), is reported and discussed elsewhere [23].

The absorption coefficient $\alpha(\omega)$ may be written as

$$\alpha(\omega) = (P_0 + P_1\omega) + \alpha_{\mathrm{tot}}F_{\mathrm{HTP}}(\omega), \tag{2}$$

where P_0 and P_1 are a pair of parameters accounting for background variations of instrumental nature, while α_{tot} is the integrated absorption coefficient.

CRDS spectra were analyzed by a Multispectrum Fitting Procedure (MFP) described in Ref. [24]. MFP allows to apply physical constraints between preselected HTP parameters leading to very accurate determinations [25]. It also reduces the statistical correlation among the parameters. Specifically, it was assumed that the collisional parameters Δ_0 and Γ_0 are linearly dependent on the pressure and, hence, on the integrated absorption coefficient α_{tot}. Conversely, since a_W and a_S can be considered constant in the entire pressure range, they were shared among the spectra. Concerning the velocity-changing collision frequency (β) and the correlation parameter (η) entering the HTP expression, we observed that, at the available SNR level, from 20 000 to 87 500, the fit quality did not improve significantly leaving β and η as free parameters or setting them to zero. This shows that in our experimental conditions the absorption spectra are well reproduced by the simpler speed-dependent Voigt profile (SDVP). A confirmation comes from the fact that the adoption of SDVP returns a physically meaningful value for a_W, namely 0.052(4), corresponding to an interaction potential of the form $1/r^q$ with an exponent q equal to about 4 [26], thus consistent with a quadrupole-dipole interaction.

MFP was applied for each data set leaving the individual temperature of the 33 spectra as a free parameter. This choice does not force a single temperature value (and thus a poor fitting quality) for spectra acquired in different days under slightly variable experimental conditions. On the other hand, the comparison between the mean temperatures of the 7 data sets is significant since the data sets virtually refer to the same temperature conditions. The absolute temperatures for each data set are reported in Fig. 3. Their standard deviation is equal to 6 mK and is consistent with the error bars provided by MFP, indicating that the temperatures retrieved are a meaningful statistical ensemble. A value of 6 mK corresponds to 20 ppm and is remarkably low if one considers that it is affected by a temperature stability of the cavity of 3 mK rms. The averaged spectroscopic temperature (298.517 K) remains offset by 10 mK (33 ppm) with respect to the averaged set-point stabilization temperature of the cavity, but such a gap minimally relates to the accuracy of the CRDS thermometer since the calibration uncertainty of the PT100 sensors was 25 mK (80 ppm).

Table I provides the uncertainty budget for the DBT determinations. The statistical uncertainty calculated as the standard deviation of the weighted mean is as low as 8 ppm over a total measurement time of ≈5 h. This value ranks among the most favorable points of the approach: as a sake of comparison, 3.2 ppm were obtained with ammonia over 70 h [27] and 15.7 ppm with water over about 50 h [9]. Due to the inverse-square-root dependence of the Type A uncertainty on the measurement time, our statistical advantage translates

TABLE I. Main uncertainty sources. Natural width, pressure leakage, and baseline distortion are excluded because of a negligible contribution (see text).

Uncertainty source	Type *A*	Type *B*
Experimental reproducibility	8 ppm	
Frequency scale uncertainty		0.5 ppm
Laser linewidth		0.2 ppm
Detector + DAQ linearity		2.3 ppm
Saturation broadening		0.3–1.6 ppm
Line-shape model		10 ppm
Doppler shift		4.8 ppm
Total uncertainty	14 ppm	

into a 2.2-fold and 38-fold reduction of the measurement time, respectively. This is highly promising to bring future DBT experiments to the 1-ppm level over practicable times. In this respect, the 6-ppm value over a "few hours" declared by Cheng *et al.* on acetylene and by CRDS [13] is a further independent indication in favor of a CRDS approach.

Concerning systematic uncertainties, negligible contributions come from the natural linewidth, which is below 1 Hz level, and from the pressure leakage, due to a minimal impact on the Gaussian part of the profile. The frequency scale uncertainty given by the GPS-disciplined clock over the 10-min time of a single DBT determination is 0.2 kHz (10^{-12}), affecting the error budget by 0.5 ppm. The linearity of detector and acquisition board were independently measured and provide a cumulative effect of 1.7×10^{-4} only at weak optical (<50 nW) and electrical (<40 mV) signals, i.e., on the part of the RD decay of less weight in the exponential fitting. This distortion translates in an uncertainty of only 2.3 ppm, thanks to the robustness given by the differential CRDS absorption law. The laser emission is relatively large (≈200 kHz linewidth), but due to its nearly Gaussian profile and to the quadrature addition law for the widths of convoluted Gaussian profiles, it affects the error budget by 0.2 ppm. Baseline distortions due to adjacent lines give a negligible contribution at the adopted pressures, where the Lorentzian term is very weak: the nearest line is 1.5 GHz apart and its strength is 5 decades lower than the $P_e(12)$ line, whereas a stronger line at the 10^{-25} cm/mol level is 8.1 GHz away. Saturation was found to have minor relevance: in fact, while being emphasized by the high finesse of the cavity and by the few-Pascal pressure range, it is mitigated by the weak Einstein coefficient (0.0078 Hz) of the transition. Specifically, a saturation broadening varying from 0.3 to 1.6 ppm depending on the pressure was calculated by an overestimated analysis where the laser was assumed steadily coupled to the cavity, with an intracavity optical power of 60 mW (which occurs only at the beginning of the RD decay) and a beam radius of 470 μm. At the lowest pressure of 1 Pa the saturation parameter amounts to 0.06%. To estimate the uncertainty given by the line-shape model we compared the mean temperature reported in Fig. 3, resulting from a SDV-profile ($\beta = 0$, $\eta = 0$), with that obtained by a more sophisticated HTP profile, where β was purposely set to the upper physically meaningful limit given by diffusion theory (1.03 MHz/Torr) and η was fixed to the 0.273 value reported in Ref. [20] for the specific CO_2 band. We found a discrepancy of 10 ppm, which may be retained as a reliable yet excess estimate for the line-shape uncertainty due to the highly different models considered.

A further uncertainty contribution comes from the Doppler shift that the intracavity field undergoes during the RD decays due to reflections from a moving mirror. This translates into a distortion of the absorption profile at the second order when the mirror speed is the same for the two motion directions and an even number of RD times are acquired and averaged together at each spectral point. To quantify the impact of this distortion on DBT experiments we made use of the numerical model discussed in Ref. [28]: from that we inferred, at each pressure value, the profile distortion and the impact on the retrieved gas temperature. The model makes use of both spectroscopic data from the sample and of experimental parameters, such as mirror speed, cavity finesse, acquisition time, and fitting procedure for the RD decays. The results show that the systematic deviation depends on pressure and that in the explored pressure range can be as high as 48 ppm. Thanks to the accurate modeling, however, its impact on the uncertainty budget remains well within 10% of the maximum deviation, which explains the 4.8 ppm value ascribed in Table I.

As a result of all factors considered in Table I, the combined uncertainty is 14 ppm, i.e., almost two times better than the best result reported so far [9]. On the statistical side, an improvement could straightforwardly result from an increased number of spectra, possibly over an even larger pressure range, whereas on the systematic side, the dominant contribution comes from the line-shape model, thus analogously to what was found in Refs. [9] and [27]. This prompts even more the identification of adequate absorption models and of reliable collisional parameters for interesting DBT candidates such as CO_2, even in the low-pressure regime here explored.

L.G. gratefully acknowledges funding from EMPIR through the project InK#2, Implementing the new Kelvin, coordinated by Graham Machin. The European Metrology Programme for Innovation and Research (EMPIR) is jointly funded by the EMPIR participating countries within EURAMET and the European Union.

[1] J. Fischer, Phil. Trans. R. Soc. A **374**, 20150038 (2016).
[2] R. M. Gavioso, D. M. Ripa, P. P. M. Steur, C. Gaiser, T. Zandt, B. Fellmuth, M. de Podesta, R. Underwood, G. Sutton, L. Pitre *et al.*, Phil. Trans. R. Soc. A **374**, 20150046 (2016).
[3] C. Gaiser, T. Zandt, and B. Fellmuth, Metrologia **52**, S217 (2015).
[4] N. E. Flowers-Jacobs, A. Pollarolo, K. J. Coakley, A. E. Fox, H. Rogalla, W. Tew, and S. Benz, Metrologia **54**, 730 (2017).
[5] C. Daussy, M. Guinet, A. Amy-Klein, K. Djerroud, Y. Hermier, S. Briaudeau, C. J. Bordé, and C. Chardonnet, Phys. Rev. Lett. **98**, 250801 (2007).
[6] E. Fasci, M. D. De Vizia, A. Merlone, L. Moretti, A. Castrillo, and L. Gianfrani, Metrologia **52**, S233 (2015).

[7] G. W. Truong, J. D. Anstie, E. F. May, T. M. Stace, and A. N. Luiten, Nat. Commun. **6**, 8345 (2015).
[8] C. H. J. Bordé, Phil. Trans. R. Soc. A **363**, 2177 (2005).
[9] L. Moretti, A. Castrillo, E. Fasci, M. D. De Vizia, G. Casa, G. Galzerano, A. Merlone, P. Laporta, and L. Gianfrani, Phys. Rev. Lett. **111**, 060803 (2013).
[10] A. Castrillo, L. Moretti, E. Fasci, M. D. De Vizia, G. Casa, and L. Gianfrani, J. Mol. Spectrosc. **300**, 131 (2014).
[11] L. Gianfrani, Phil. Trans. R. Soc. A **374**, 20150047 (2016).
[12] A. Cygan, D. Lisak, S. Wójtewicz, J. Domysławska, J. T. Hodges, R. S. Trawinski, and R. Ciuryło, Phys. Rev. A **85**, 022508 (2012).
[13] C. F. Cheng, J. Wang, Y. R. Sun, Y. Tan, P. Kang, and S. M. Hu, Metrologia **52**, S385 (2015).
[14] J. Burkart, D. Romanini, and S. Kassi, Opt. Lett. **39**, 4695 (2014).
[15] D. Gatti, R. Gotti, A. Gambetta, M. Belmonte, G. Galzerano, P. Laporta, and M. Marangoni, Sci. Rep. **6**, 27183 (2016).
[16] R. Gotti, D. Gatti, P. Maslowski, M. Lamperti, M. Belmonte, P. Laporta, and M. Marangoni, J. Chem. Phys, **147**, 134201 (2017).
[17] L. S. Rothman, I. E. Gordon, Y. Babikov, A. Barbe, D. Chris Benner, P. F. Bernath, M. Birk, L. Bizzocchi, V. Boudon, L. R. Brown *et al.*, J. Quant. Spectrosc. Radiat. Transfer **130**, 4 (2013).
[18] M. D. De Vizia, F. Rohart, A. Castrillo, E. Fasci, L. Moretti, and L. Gianfrani, Phys. Rev. A **83**, 052506 (2011).
[19] D. Lisak, J. T. Hodges, and R. Ciuryło. Phys. Rev. A **73**, 012507 (2006).
[20] G. Larcher, X. Landsheere, M. Schwell, and H. Tran, J. Quant. Spectrosc. Radiat. Transfer **164**, 82 (2015).
[21] J. Tennyson, P. Bernath, A. Campargue *et al.*, Pure and Appl. Chem. **86**, 1931 (2014).
[22] H. Tran, N. H. Ngo, and J.-M. Hartmann, J. Quant. Spectrosc. Radiat. Transf. **134**, 104 (2014); Erratum to: J. Quant. Spectrosco. Radiat. Transf. **129**, 199 (2013).
[23] M. D. De Vizia, A. Castrillo, E. Fasci, P. Amodio, L. Moretti, and L. Gianfrani, Phys. Rev. A **90**, 022503 (2014).
[24] P. Amodio, L. Moretti, A. Castrillo, and L. Gianfrani, J. Chem. Phys. **140**, 044310 (2014).
[25] P. Amodio, M. D. De Vizia, L. Moretti, and L. Gianfrani, Phys. Rev. A **92**, 032506 (2015).
[26] C. H. Townes and A. L. Schawlow, *Microwave Spectroscopy* (Dover, Mineola, NY, 1955).
[27] C. Lemarchand, M. Triki, B. Darquié, Ch. J. Bordé, C. Chardonnet, and C. Daussy, New J. Phys. **13**, 073028 (2011).
[28] D. Gatti, T. Sala, R. Gotti, L. Cocola, L. Poletto, M. Prevedelli, P. Laporta, and M. Marangoni, J. Chem. Phys. **142**, 074201 (2015).